The energy dissipation during fatigue crack growth in adhesive joints under Mode-I loading
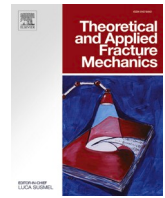
Quan, H.; Alderliesten, R. C.

Important note
To cite this publication, please use the final published version (if applicable).
Please check the document version above.

The energy dissipation during fatigue crack growth in adhesive joints under Mode-I loading

H. Quan [*], R.C. Alderliesten

Structural Integrity & Composites, Faculty of Aerospace Engineering, TU Delft, Netherlands

ABSTRACT

An energy equation for fatigue crack growth in adhesive joints is proposed. Fatigue experiment on DCB adhesive joint specimens was used to derive the relation between fatigue crack growth rate (da/dN) and energy variables in this equation. The result shows plastic dissipation and change in stored strain energy, whose relation with da/dN both depending on the stress ratio, are not straightforwardly related to da/dN. The energy dissipated in new crack surface formation is the variable that straightforwardly related to da/dN within the range of test, and its relation with da/dN is one-to-one, regardless of the influence of stress ratio.

1. Introduction

The adhesive joint has been used for decades as an alternative to mechanical fastening for weight reduction purposes in aerospace structures, as it provides a more uniform stress distribution by avoiding stress concentrations caused by the fastening holes. Currently the fatigue failure is one typical failure mechanism in adhesive joints in engineering practices. Therefore, a good understanding of the fatigue phenomenon and a validated prediction method for fatigue damage growth in adhesively bonded structures are highly important for engineers at the designing stage to avoid catastrophic consequences in the future.

Nowadays, most practice on the research on fatigue crack growth in adhesive joints has been carried out within the scope of fracture mechanics [1–10]. The variables from fracture mechanics: ΔG, G_{max} and $\Delta\sqrt{G}$, are used as the similitude to describe and predict the fatigue crack growth in adhesive joints. The engineering practice using ΔG, G_{max} and $\Delta\sqrt{G}$ is successful, although from a physics perspective, the physical meaning of some fracture mechanics variables are questionable. Fig. 1 explains energy dissipation during one load controlled cycle of fatigue crack growth in brittle materials. The real energy dissipated by fatigue crack growth is defined by the load–displacement hysteresis as shown in Fig. 1 (a). However, the values of strain energy release rate range multiplied by fatigue crack growth rate $\Delta G(da/dN)$ and maximum strain energy release rate multiplied by fatigue crack growth rate $G_{max}(da/dN)$, as shown in Fig. 1 (b) and (c), are different from the real energy dissipated by fatigue crack growth. The actual energy dissipated by unit fatigue crack propagation is different from ΔG and G_{max}. Therefore, the fracture mechanics variables used as similitude: ΔG and G_{max}, cannot represent the actual energy dissipation for fatigue crack propagation.

To explain this, we have to revisit the fracture mechanics framework to study fatigue crack growth in adhesive joints, as illustrated in Fig. 2. Historically, for the research of static crack growth, Griffith [11] and Irwin [12] studied the static crack growth with energy-based concepts from physics. Based on the energy concepts, the strain energy release rate G was defined as the strain energy release caused by infinitely small crack increment under fixed grip conditions, where the total energy of the system remains and the strain energy release is available for crack growth. Therefore, G can be considered as the driving force only when the priori of static crack is met. For static crack growth, G was related to the resistance of the material, as $G > G_c$ in engineering practice. The history of the study of static crack growth follows a normal order of research: firstly studying the phenomenon from a scientific view to obtain the objective law behind it, and then application to engineering practice based on the knowledge acquired. However, this is not the case for the study of fatigue crack growth. G for static crack growth is taken over into different forms as driving force for fatigue crack growth, without starting to analyse fatigue crack growth from a physics view at first. Directly using G in fatigue cannot meet the priori of static crack, violating the concept of Griffith. Therefore, violating Griffith's condition in applying G from static to fatigue without considering the priori, likely invalidates the current fracture mechanics variables used for fatigue crack growth in a physics perspective.

The physics underlying fatigue crack growth in adhesive joints is overlooked, illustrated by the question mark in Fig. 2, for limited

---

literature can be found on this topic. Pascoe [13] correlated the release of strain energy with fatigue crack growth rate in adhesive joints, but a comprehensive overview of what energy components are involved and what role these energy components play in fatigue crack growth in adhesive joints is lacking. The fatigue damage growth in different material systems, such as fatigue crack growth in metals and fatigue delamination growth in composites, are in fact the same phenomenon in physics perspective. So the research work on other material systems should give us new insights on the study of fatigue crack growth in adhesive joints. For fatigue crack growth in metallic materials, the relation between plastic dissipation and da/dN was studied in [14–21]. The relation between the strain energy release and fatigue delamination growth rate in composites were studied under Mode I [22–23], Mode II [24] and mixed mode [25]. Consequently, for the adhesive joints with ductile adhesive materials, both the plastic dissipation and the strain energy release should be taken into account for the scientific stage study on the fatigue crack growth in adhesive joints.

The purpose of this paper is to study the fatigue crack growth in adhesive joints from a physics perspective on energy to fill the missing part of our knowledge, identified with question mark in Fig. 2. Therefore, the main questions addressed in this paper are:

1. What energy components are involved during fatigue crack growth in adhesive joints?
2. What role do all these energy variables play and which one is straightforwardly related to da/dN?

2. The energy balance for fatigue crack growth in adhesive joints

The fatigue crack growth in adhesive joints is analysed here with an energy approach stemming from physics. First, as an analogy to fatigue crack growth, the static crack growth can be described with an energy equation as [26]:

$$\dot{W} = \dot{U}_e + \dot{U}_{pl} + \dot{U}_a \qquad (1)$$

where $\dot{U}_e$ is the change in the stored elastic strain energy, and $\dot{U}_{pl}$ is the plastic dissipation. $\dot{U}_a$ is the surface energy dissipated through the formation of new crack surfaces, and $\dot{W}$ is the external work done to the cracked body. Reference [26] considers the surface formation energy as the driving force of crack growth. In this case, it is reasonable to assume that $\dot{U}_a$ is straightforwardly related to crack growth, while it is unclear whether $\dot{U}_e$ and $\dot{U}_{pl}$ are also straightforwardly related to crack growth.

Similarly, the energy equation for fatigue crack growth can be written discretized per load cycle as:

$$\frac{dW}{dN} = \frac{dU_e}{dN} + \frac{dU_{pl}}{dN} + \frac{dU_a}{dN} \qquad (2)$$

where dW/dN is the external work done to the cracked body from outside over a full cycle, and dU_e/dN is the change in the elastic strain energy stored throughout one full cycle. dU_{pl}/dN is the plastic dissipation per cycle, and dU_a/dN is the surface energy dissipated thorough new fatigue crack surface formation. The left side of this equation is the energy input from outside and the right side of the equation are the corresponding energy stored and energy dissipated within the cracked body. A similar equation is reported in [27] for fatigue crack growth in coatings. Similar to static crack growth, it is logical to assume that dU_a/dN is straightforwardly linked to fatigue crack surface area growth dA/dN. A is the true fatigue crack surface area in rough fracture surfaces, which is not the planar projection area defined by the crack length a multiplied by the thickness (for DCB specimen: width). However, because the true crack surface area is difficult to measure, the fatigue crack length is used as first approximation to correlate with the energy variables. Equation (2) is obtained based on the framework of classical elastic plastic fracture mechanics by Rice and Newman, so the equation may not be complete to consider all the dissipation mechanics. For example, crack surface contact shielding (like friction between crack surfaces) could also be added to the equation. But for the first step trail, this paper still keeps in the classical elastic plastic fracture mechanics by Rice and Newman. Similar to Fig. 1, the energy variables in Equation (2) could be illustrated in Fig. 3 for brittle materials whose $\frac{dU_{pl}}{dN} \approx 0$. In Fig. 3, the fatigue cycle is from the N_{th} minimum load to $(N + 1)_{th}$ minimum load. If considering the plastic dissipation for ductile materials, the dU_{pl}/dN should also be included in the hysteresis in the right figure of Fig. 3.

If one energy variable is straightforwardly linked to fatigue crack growth, the quantitative relationship between da/dN and this energy variable should be a one-to-one relationship, regardless of the external loading conditions, such as the stress ratio. Therefore, if the assumption of dU_a/dN straightforwardly linked to fatigue crack growth is correct, the dU_a/dN-da/dN relationship should be a one-to-one relationship, regardless of the stress ratio. Meanwhile, if the dU_e/dN-da/dN relationship and the dU_{pl}/dN-da/dN relationship depend on the stress ratio, then dU_e/dN and dU_{pl}/dN are just the consequences accompanying fatigue crack propagation, not straightforwardly linked to fatigue crack growth.

3. Method for obtaining da/dN and energy variables

Fatigue experiments were carried out to obtain the energy variables in correlation with da/dN to validate the previous assumption of dU_a/dN straightforwardly related to da/dN. The Mode I Double cantilever beam
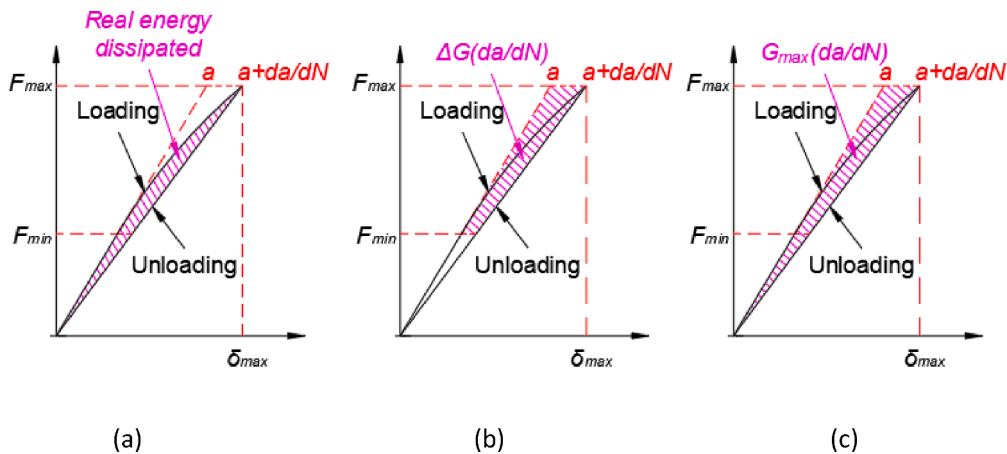

Fig. 1. ΔG and G_{max} cannot represent the real energy dissipation for fatigue crack propagation.

(DCB) fatigue tests with metal-to-metal adhesive joints were carried out and the values of dU_e/dN were measured experimentally. The values of dU_{pl}/dN were obtained by finite element analysis (FEA). The values of dU_a/dN were obtained with both FEA simulation and an analytical approach.

3.1. Fatigue experiments description

The fatigue tests were performed on the DCB metal-to-metal adhesive joints specimens. The adhesive used is Cytec FM94, and the adherend material is 7075-T6. The specimens were manufactured by bonding two 7075-T6 plates with two layers of FM94 film adhesive with polyester carrier. The 7075-T6 surfaces for bonding were pre-treated with the procedure of solvent degreasing, alkaline cleaning, chemical deoxidizing and primer application with BR 6747–1 primer. A layer of release film was applied in a portion of surfaces for bonding to create the initial crack. The adhesive was cured in the autoclave under 0.28 MPa pressure with vent vacuum at 0.14 MPa. For the curing cycle, first the temperature was raised to 121 °C in 50 min, and then the temperature was maintained at 121 °C for 1 h. Finally, the temperature was cooled down in 50 min with pressure holding. After curing, the plates were cut into the final dimensions of the test specimens, as shown in Fig. 4. After curing the bond-line thickness was measured with Keyence optical microscope and the thickness is 0.26 mm ± 0.012 mm.

The fatigue tests were performed displacement controlled on an MTS 15kN fatigue machine with 1kN load cell. The load was recorded by the 1kN load cell of the fatigue machine, and the crack length was measured by one 4Mpix camera on the side of the specimens, with the resolution not lower than 25 pixel/mm, so the error of crack length measurement is below 0.04 mm. The displacement was measured by Vic-3D digital image correlation (DIC) system with a pair of 80 mm lenses and 5Mpix cameras, with a resolution of about 70 pixel/mm. The displacement was measured from the side surfaces of the DCB specimens instead of taken from the fatigue machine for 2 reasons. First, with DIC the displacement measurement can be more accurate. Second, the displacement measurement is directly from the test specimens, without the interference of the fixture or test machine. Thus, the measured displacement is the pure surface separation of DCB specimen, and the energy variables calculated from the DIC displacement later in this paper can exclude the influence of fixture. At the first 10,000 cycles, the measurement data of crack length, minimum and maximum displacement, and minimum and maximum load of one cycle were recorded once in every 200 cycles. After that the data of crack length, minimum and maximum displacement, and minimum and maximum load were recorded once every 2000 cycles.

Different stress ratios were achieved by different ratios of minimum displacement to maximum displacement of the fatigue machine in one cycle d_{min}/d_{max}, of which two were tested, $d_{min}/d_{max} = 0.15$ and 0.5. For each stress ratio six specimens were tested. The average stress ratios measured by the load cell were $R = 0.13$ for $d_{min}/d_{max} = 0.15$ and $R = 0.47$ for $d_{min}/d_{max} = 0.5$. The frequency was 3 Hz in all tests. The fatigue crack growth rate da/dN was calculated by incremental polynomial method [28] from the crack lengths measured from the photos taken by the 4Mpix camera at different numbers of cycles.

3.2. The measurement of dU_e/dN

The values of dU_e/dN were calculated by incremental polynomial method from the elastic strain energy at different numbers of cycles. The elastic strain energy was calculated from the load and displacement measurement recorded at different cycles.

First, the stiffness for the DCB specimen was calculated with $K = \Delta F/\Delta d$, where ΔF is the maximum force minus minimum force in one cycle, and Δd is the maximum displacement from DIC minus minimum displacement from DIC in one cycle. The elastic strain energy U_e at different numbers of fatigue cycles N was calculated from the stiffness and the corresponding force F: $U_e = F^2/2k$. Finally dU_e/dN was obtained by U_e at different numbers of fatigue cycles N by incremental polynomial method in [28].

3.3. FEA simulation to obtain dU_{pl}/dN and dU_a/dN

The values of dU_{pl}/dN and dU_a/dN were obtained through FEA simulation, because quantitatively they are too small to be measured in the tests. The plastic dissipation is only in adhesive, while the 7075-T6 adherend maintains purely elastic during the test.

The DCB specimen was simulated with a half model using symmetry conditions for Mode I crack. The fatigue crack growth was simulated by node release technique and the model was in 2D plane strain condition. The boundary conditions for the FEA model is illustrated in Fig. 5(a). The symmetrical boundary condition was applied at the bottom to simulate the uncracked region. The displacement in X-direction of the top-left point of the FEA model was constrained and the displacement in Y-direction was applied at this point to simulate the cyclic displacement by the fatigue machine, making the FEA model displacement controlled. The crack surface was simulated as free surface, and a rigid line was placed at the crack surface position to account for crack closure. Surface to Surface contact was set between crack surface and rigid line with the contact properties of hard contact in normal direction and frictionless in tangential direction. The 4-node bilinear plane strain element was used
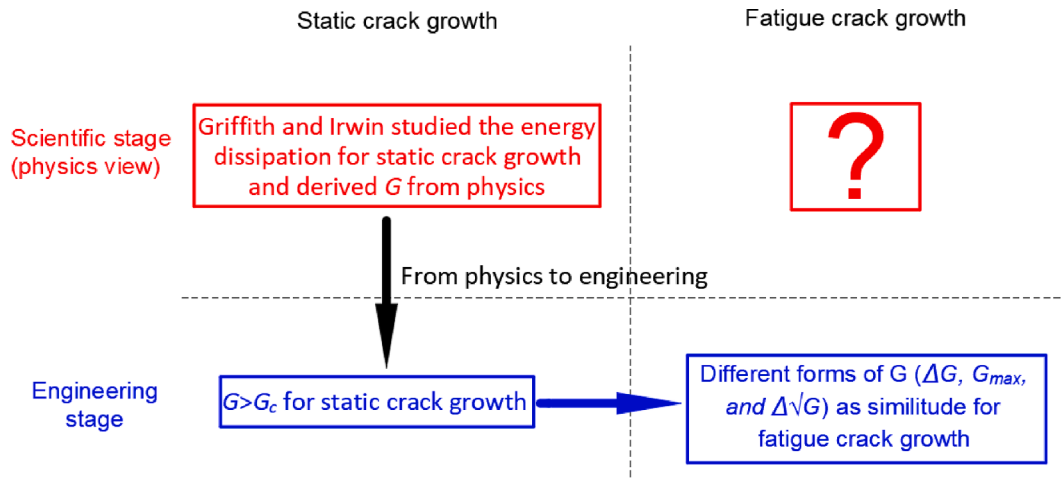

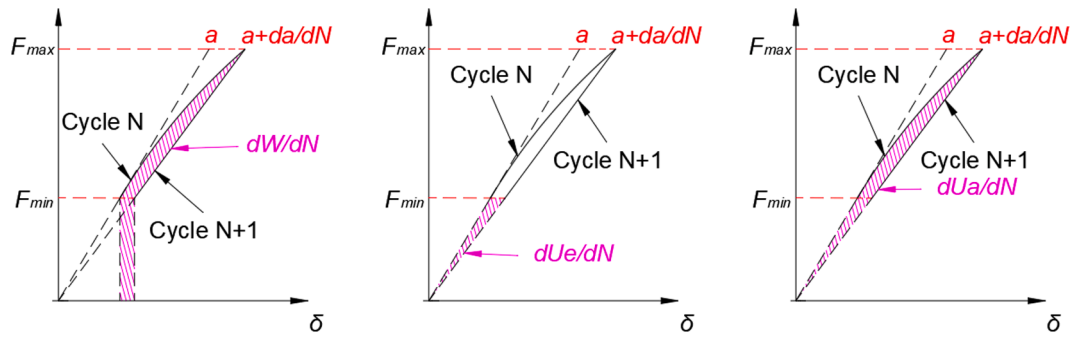**Fig. 2.** Framework to evaluate fatigue crack growth in adhesive joints.

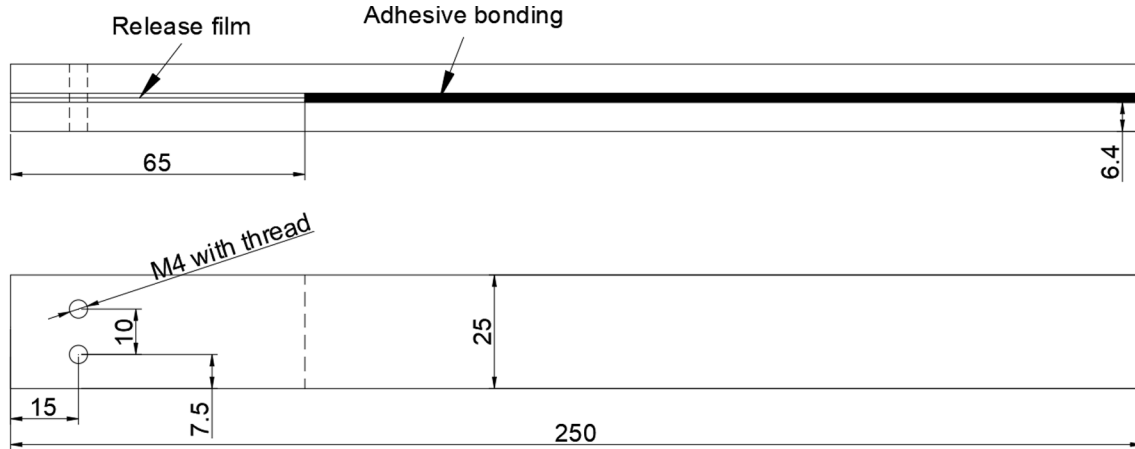**Fig. 3.** Energy variables in Equation (2) for brittle materials.

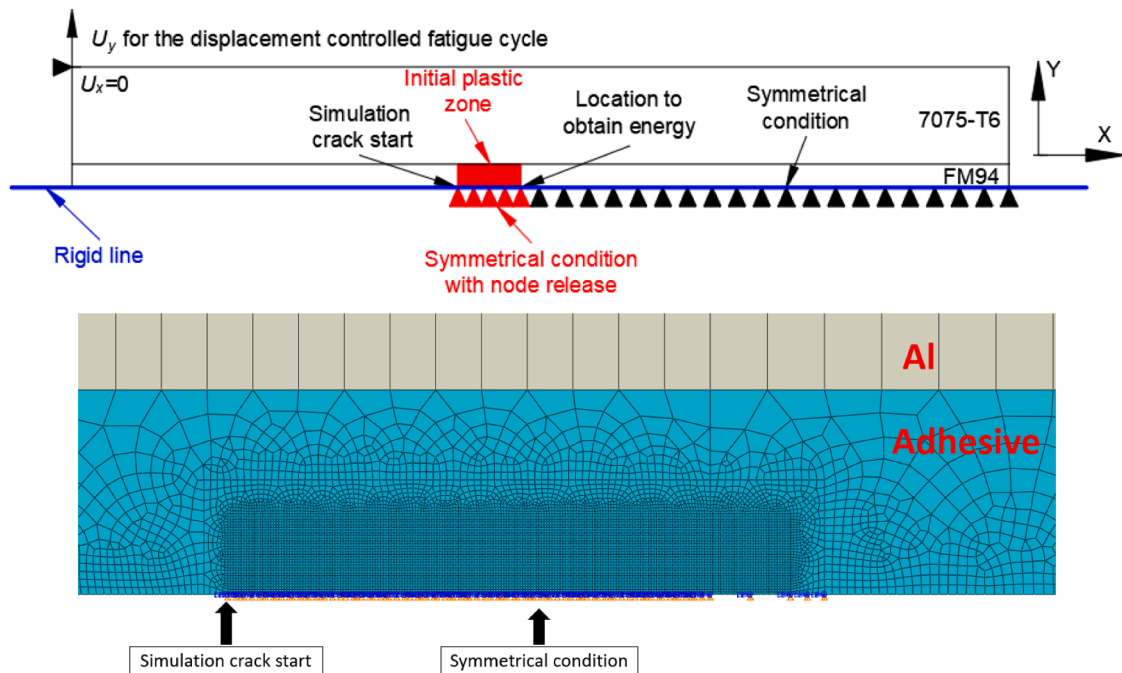**Fig. 4.** Dimensions of fatigue test specimens.

Fig. 5. (a). Illustration of the FEA model of the DCB specimen (not drawn to scale) Fig. 5(b). Mesh around crack in the FEA model of the DCB specimen.

in simulation and the simulation was performed in ABAQUS standard. The adhesive and adherend were simulated with a whole part containing different material properties in the different regions of the part. 7075-T6 was pure elastic in simulation with the elastic modulus $E = 69200$ MPa

and the Poisson ratio 0.33. FM94 was simulated with elasto-plastic model with the elastic modulus of $E = 2355.4$ MPa and the Poisson ratio 0.4 as in [29]. The nonlinear kinematic hardening model was used to model the plastic region of FM94, as the shear stress–strain

relationship of FM94 in Fig. 6. This shear stress–strain relationship of FM94 is from the V-notched beam shear tests reported in [29].

The simulation is to obtain the theoretical dU_a/dN at a given da/dN, rather than validating any fatigue crack growth criterion used in FEA by comparing the simulation results with experimental results. So it is important to ensure the fatigue crack extends a given da/dN for every fatigue cycle. In fact, the da/dN can be retrieved from fatigue experiments described in Section 3.1, and fatigue crack growth can be simulated by node release in every cycle discretely. In this case, the dU_a/dN at a given da/dN has a clear meaning and definition in simulation. There are two patterns of fatigue crack growth used in simulation in this paper, as in Fig. 7. Pattern A assumes all fatigue crack propagating at the maximum displacement. Pattern B assumes equal fatigue crack increments at 3 displacement levels: d_{max}, d_2, d_1, respectively. d_2 and d_1 were arbitrarily chosen to see the influence of crack propagation pattern during one cycle. In this paper, $d_1 = 0.5(d_{max} + d_{min})$ and $d_2 = 0.5(d_{max} + d_1)$.

A very fine mesh was set in the adhesive layer around crack tip, and coarser mesh was set in the region away from crack tip, as shown in Fig. 5(b). The mesh size around crack is less than 1/6 of the reversed plastic zone size, which is smaller than the bond line thickness. The element sizes around crack are different for every FEA models used in simulation to simulate different da/dN for different FEA models. Both the values of dU_{pl}/dN and dU_a/dN were obtained when the fatigue crack propagating through the initial plastic zone generated in the first cycle at the maximum load, to account for the effect of the initial plastic field. The shape and the size of the initial plastic zone generated in the first cycle at the maximum load is decided by the simulation of the FEA model with static crack before performing the simulation of fatigue crack growth. The crack propagating at the first cycle or not has little influence in this simulation, because the energy variables are obtained after the crack propagating through the initial plastic zone and the da/dN used in simulation is far less than the initial plastic zone size.

The dU_a/dN values were obtained from the difference between the external work from fatigue loading and the internal energy, including elastic strain energy and plastic dissipation, from the FEA model, because there is no other dissipation mechanics except for the plastic dissipation, surface formation and elastic strain energy storage in simulation. Friction can be ignored in simulation because of the symmetrical condition for Mode I crack. The dU_a/dN can be calculated as:

$$\frac{dU_a}{dN} = \int Fd\delta - \frac{d(ALLIE)}{dN} + \left[\frac{d(ETOTAL)}{dN} + \frac{d(ALLCCDW)}{dN} - \frac{d(ALLCCE)}{dN}\right]$$
(3)

where F and δ are the load and displacement for the loading point. $\int Fd\delta$ is the theoretical external work throughout one fatigue cycle defined by the load–displacement hysteresis. $ALLIE$ is the ABAQUS output for internal energy. $\left[\frac{d(ETOTAL)}{dN} + \frac{d(ALLCCDW)}{dN} - \frac{d(ALLCCE)}{dN}\right]$ is the numerical error in
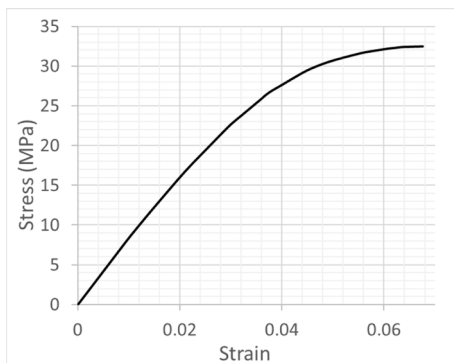

Fig. 6. Shear stress–strain relationship of FM94.

ABAQUS. $ETOTAL$ represents the error from the solver. $ALLCCDW$ is contact constraint discontinuity work and $ALLCCE$ is contact constraint energy, both representing the numerical error caused by contact in ABAQUS. The term for numerical error in simulation was included because dU_a/dN is very small and eliminating numerical error can provide more accurate results.

The numerical dU_a/dN values highly depend on the crack surface newly formed by the crack extension in one fatigue cycle in simulation, so for each crack extension enough elements should be included in the newly formed crack surface. A convergence study with different FEA models with the same simulated da/dN and boundary conditions in simulation, but with different element sizes around crack, was made and it was concluded that six elements could yield good convergences for both Pattern A and B. Therefore, six nodes were released for each fatigue crack extension in the FEA simulation. The da/dN used in simulation is six times of the element size around crack tip for Pattern A, and 18 times of the element size around crack tip for Pattern B. However, the element size cannot be small enough to simulate the real da/dN in the experiments, because too small element will cause numerical problems. To solve this, an extrapolation to the experimental da/dN based on the relationship between dU_a/dN simulation results and the da/dN used in simulation was applied as Fig. 8.

For a specific moment during the fatigue test, the corresponding boundary conditions needed for simulation (crack length a, max displacement d_{max} and R) and experimental da/dN can be retrieved from experimental data recorded. For this specific moment, the corresponding FEA models are with the same boundary conditions to simulate the same loading condition in experiments, but with different element sizes around crack for different simulated da/dN in FEA. The dU_a/dN simulation results of this specific moment with different da/dN used in simulation can be obtained from these FEA models, as the black dots in Fig. 8. The relationship between simulation dU_a/dN values and different da/dN used in simulation was fitted with a power law accurately as the blue line. The dU_a/dN value for this specific moment in test with experimental da/dN was obtained by applying the experimental da/dN into this power law fitted from simulation data as Fig. 8. Following the same method, the actual dU_a/dN values corresponding to different moments in experiments with their corresponding experimental da/dN can be obtained. The actual dU_a/dN at a different moment during the fatigue test can be extrapolated from the simulation results of the FEA models with different element sizes under the same boundary condition at this different moment.

After the crack tip propagating through the initial plastic zone in the first cycle, 6 stable fatigue cycles with stationary crack without crack extension were used to obtain the values of dU_{pl}/dN, similar to [16–17], because the influence of experimental da/dN on plastic dissipation is negligible. A convergence study was made that demonstrated that the numerical dU_{pl}/dN converges with decreasing element size in the crack tip region and the pattern of fatigue crack growth in simulation has negligible influence on numerical dU_{pl}/dN with good mesh density. This convergence value of dU_{pl}/dN is taken as the final numerical dU_{pl}/dN result for a given loading condition.

To provide more information on dU_a/dN, the FEA simulation was also performed with compact tension (CT) specimen only containing the bulk adhesive material. The CT specimen geometry for simulation follows ASTM standard E647 [28] with $W_{ct} = 100$ mm and crack length $a = 50$ mm. The da/dN for CT specimens should be approximately the same as the da/dN for DCB specimens at the same ΔG and R, according to the knowledge of fracture mechanics. The simulation was in plane-strain condition with half model, because of the symmetrical Mode I crack. The FEA model for the CT specimen is illustrated in Fig. 9. The numerical values of dU_a/dN for the CT specimen were obtain with the same method for obtaining the numerical values of dU_a/dN for the DCB specimen, as previously described.

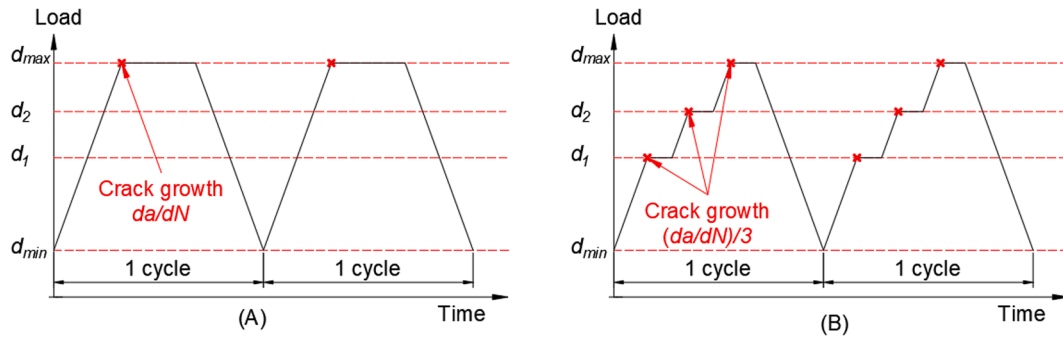The previous assumption of dU_a/dN straightforwardly linked to $da/$

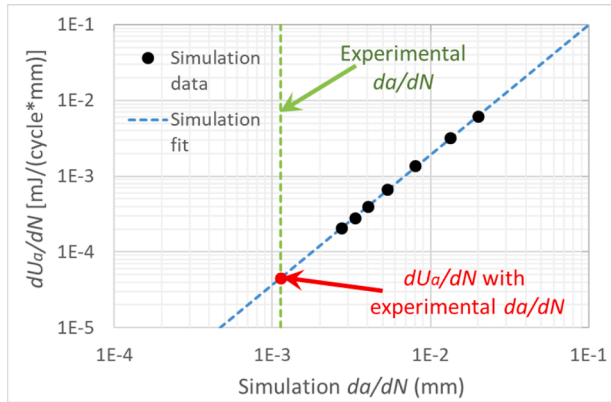**Fig. 7.** Two patterns of fatigue crack growth used in simulation.

Fig. 8. Extrapolation to obtain dU_a/dN at experimental da/dN ($R = 0.47$, max displacement 2.66 mm, $a = 100$ mm, Pattern A).

dN can be supported, if the dU_a/dN-da/dN relationship of CT specimen is the same as the dU_a/dN-da/dN relationship of DCB specimen, regardless of the specimen type. The results with different specimen types are presented and discussed further in 4.3 in this paper.

3.4. Analytical approach to obtain dU_a/dN

To verify the FEA simulation for obtaining dU_a/dN, another analytical approach is presented here. This approach is based on the strip yield model of fatigue crack growth in central crack panel in plane-strain condition, for which details are reported in [30]. This strip yield model was programmed in Matlab. Similar to the FEA simulation, both Pattern A and B for fatigue crack growth in Fig. 7 were used in the strip yield model. After the fatigue crack propagating through the initial

plastic zone generated in the first cycle at the maximum load, the values dU_a/dN were obtained to account for the effect of the initial plastic field. The concept for fatigue crack extension in the strip yield model is illustrated in Fig. 10. The surface formation energy for each crack extension ΔU_a (per unit thickness) was obtained following the same concept as the virtual crack closure technique (VCCT), as in Equation (4):

$$\Delta U_a = \int_a^{a+\Delta a} \sigma_Y(x)v(x)dx \tag{4}$$

where $\sigma_Y(x)$ is the vertical stress distribution, which can be retrieved from the stress calculation results of the strip yield model. $v(x)$ is the vertical displacement of the crack surface, which is obtain from the calculation of the strip yield model. The $v(x)$ is calculated by the fictitious crack surface vertical displacement of the strip yield model minus the residual plastic deformation of the bar elements of the strip yield model. More detail can refer to [30]. The dU_a/dN for pattern A is the ΔU_a calculated at the maximum load. The dU_a/dN for pattern B is the sum of three ΔU_a values calculated at 3 different load levels for crack extension. The da/dN in the analytical approach can be as small as the experimental da/dN, without the need to extrapolate as in the FEA simulation. However, the values of dU_a/dN depend on the element size in the strip yield model, similar to FEA simulation. Therefore, a convergence study was made and the results illustrated that a crack propagating six elements for each crack extension in the analytical approach gives good convergence. Therefore, the element size of this analytical approach is 1/6 of the experimental da/dN for pattern A, and 1/18 of the experimental da/dN for pattern B.

4. Results and discussion

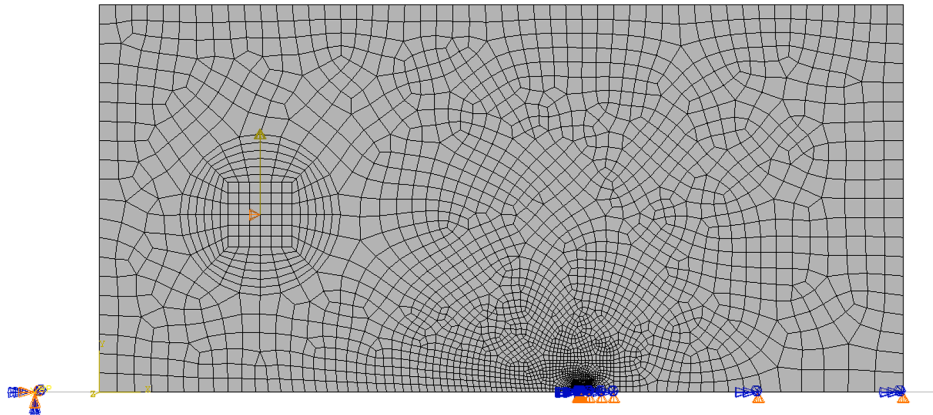The experimental fatigue crack growth rate da/dN is plotted against

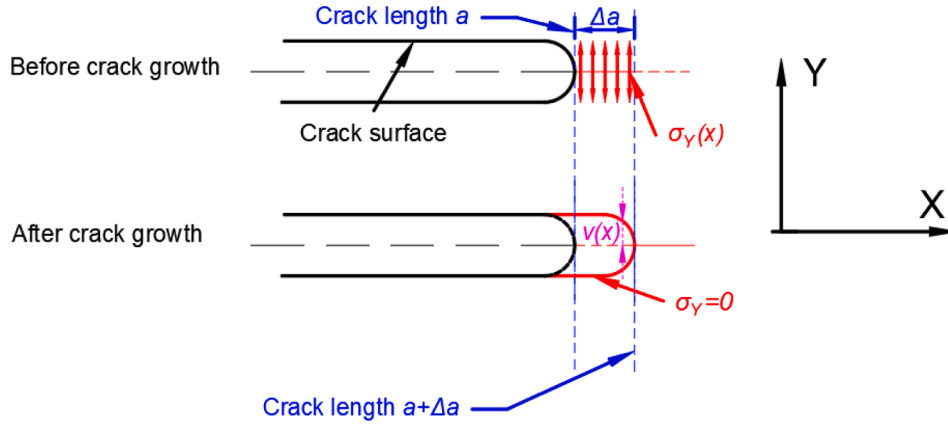**Fig. 9.** Illustration of the FEA model of the CT specimen.

Fig. 10. Fatigue crack extension in strip yield model.

$\Delta\sqrt{G}$ in Fig. 11. These experimental results agree with [31–34]. After this initial verification, the next step was to study the relationship between da/dN and different energy variables. All the energy variables for DCB specimen presented in this paper are normalized to the DCB specimen width of 25 mm unless otherwise specified.

4.1. The relation between dU_e/dN and da/dN

The values of dU_e/dN depend strongly on the definition of the starting point of the fatigue cycle. For instance, two typical dU_e/dN values can be obtained for the conditions that the fatigue cycle is from the maximum load to next maximum load (max-max) and from the minimum load to next minimum load (min-min). The values of dU_e/dN of min-min condition are significantly smaller than the values of max-max condition. Therefore, the results of both conditions are presented here.

The values of dU_e/dN can be estimated with an analytical approach. For unit width of DCB specimen under static load, the energy release rate G is:

$$G = \frac{dU_e}{da} \tag{5}$$

Similarly, in fatigue loading at the maximum load:

$$G_{max} = \frac{dU_e/dN}{da/dN} \tag{6}$$

Thus the analytical estimation of dU_e/dN for max-max condition is $G_{max}(da/dN)$. Similarly, the analytical estimation of dU_e/dN for min-min condition is $G_{min}(da/dN)$. The comparison between the experimental measurement and analytical estimation is presented in Fig. 12. Good
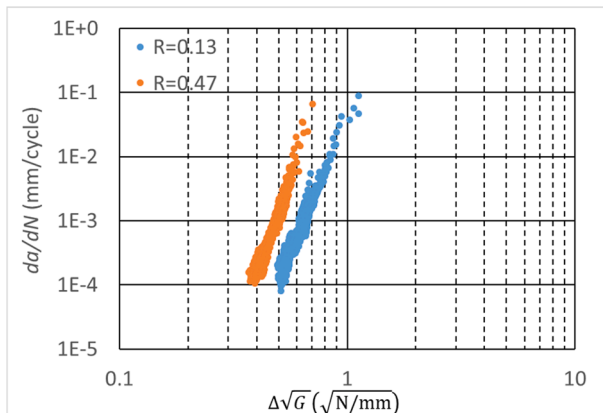
agreement can be observed between estimation and the experimental measurements.

The dU_e/dN - da/dN relationship is presented in Fig. 13. From this figure, it can be concluded that the dU_e/dN - da/dN relationship depends on the stress ratio, for both min-min and max-max conditions. This stress ratio dependence of the dU_e/dN - da/dN relationship can be explained with the G in Equation (6). The values of G are different for different stress ratios at the same da/dN. Meanwhile, theoretically the starting point of one fatigue cycle can be any point between maximum load and minimum load, so for the same fatigue cycle, dU_e/dN can be any value between dU_e/dN for max-max condition and dU_e/dN for min-min condition. The chaos in the definition of dU_e/dN makes dU_e/dN impractical to correlate with da/dN. Therefore, the dU_e/dN - da/dN relationship depends on the stress ratio, meaning dU_e/dN is just the consequence accompanying fatigue crack propagation and it is not straightforwardly linked to fatigue crack growth as previously assumed.

4.2. The relation between dU_{pl}/dN and da/dN

The plastic dissipation per cycle during fatigue crack propagation in DCB specimens dU_{pl}/dN is plotted in Fig. 14 against $\Delta\sqrt{G}$. From Fig. 14, it is observed that compared with the da/dN-$\Delta\sqrt{G}$ relationship, the dU_{pl}/dN-$\Delta\sqrt{G}$ relationship shows little stress ratio dependence. Similar results are reported in [35–37] for fatigue crack growth tests in metals, where the dU_{pl}/dN-ΔK relation from experiments has negligible stress ratio effect. Because $\Delta\sqrt{G}$ is proportional to ΔK, it is reasonable that the dU_{pl}/dN-$\Delta\sqrt{G}$ relationship here has little stress ratio effect as well.

The relation between dU_{pl}/dN and da/dN is shown in Fig. 15, from which one can observe that the relation between dU_{pl}/dN and da/dN has a strong stress ratio dependence. Therefore, dU_{pl}/dN is just the consequence accompanying fatigue crack propagation and it is not straightforwardly linked to fatigue crack growth.

4.3. The relation between dU_a/dN and da/dN

The relation between dU_a/dN and da/dN is plotted in Figs. 16-17. The annotations of "DCB" in Figs. 16-17 mean dU_a/dN was obtained by the extrapolation of FEA simulation of DCB specimens. The annotations of "CT" in Fig. 16 mean dU_a/dN was obtained by the extrapolation of FEA simulation of CT specimens. The annotations of "Analytical" in Figs. 16-17 mean dU_a/dN was obtained based on the analytical approach with strip yield model as Equation (4).

Although quantitatively the dU_a/dN values are different for Pattern A and B in Figs. 16-17, the trend of dU_a/dN remains the same, thus different patterns of fatigue crack growth used in this paper in simulation do not influence the dU_a/dN trend. From Figs. 16-17, it can be observed that dU_a/dN-da/dN relationship is independent of the stress
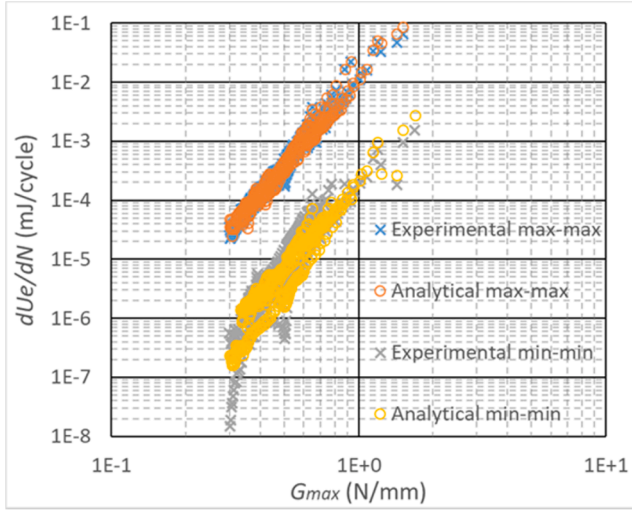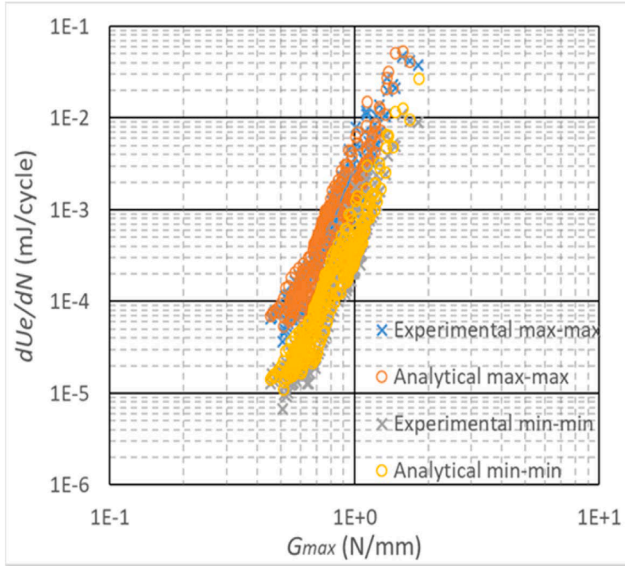

Fig. 11. Experimental da/dN plotted against $\Delta\sqrt{G}$ for two stress ratios R.

(a) *R*=0.13

(b) *R*=0.47

Fig. 12. The comparison between the experimental measurement and analytical estimation.

ratio. The dU_a/dN obtained with the FEA simulation shows good agreement with dU_a/dN obtained with the analytical approach in both Figs. 16-17, which essentially validates the current results. Meanwhile, as in Fig. 16, the dU_a/dN-da/dN relationship for DCB specimens agrees with the dU_a/dN-da/dN relationship for CT specimens, meaning that the relation between dU_a/dN and da/dN is independent of the type of specimen as well. Therefore, dU_a/dN should be the variable straightforwardly linked to da/dN, unlike dU_{pl}/dN and dU_e/dN, for that the dU_a/dN-da/dN relationship is independent of both specimen type and stress ratio.

5. Conclusion

A physics based equation for fatigue crack growth in adhesively bonded joints is reported in this paper. This equation shows the balance between the energy input and the sum of stored energy and dissipation: the external work throughout the whole cycle dW/dN is equal to the sum
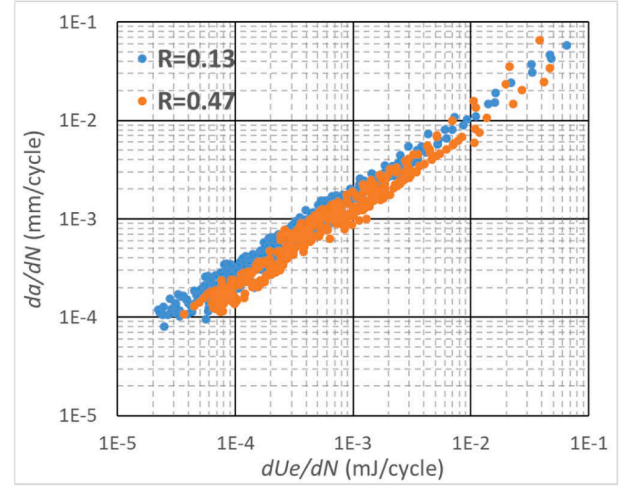
(a) max-max
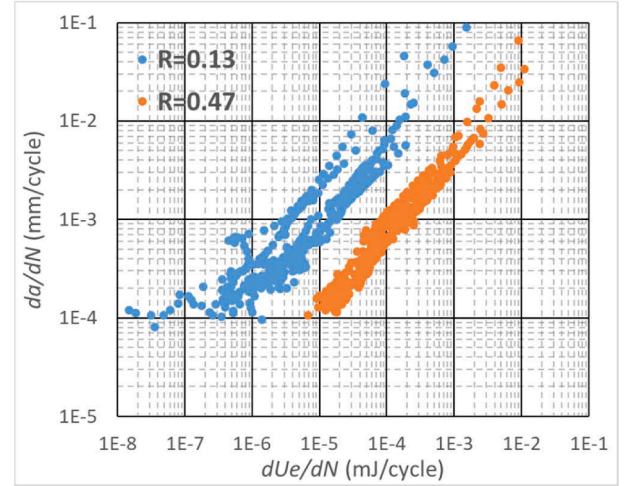
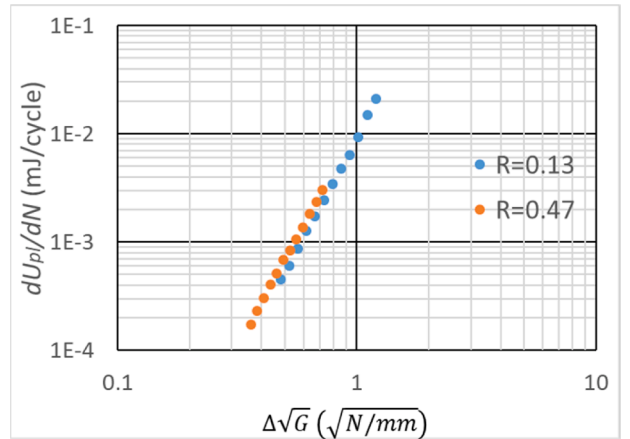
(b) min-min

Fig. 13. The dU_e/dN - da/dN relationship.

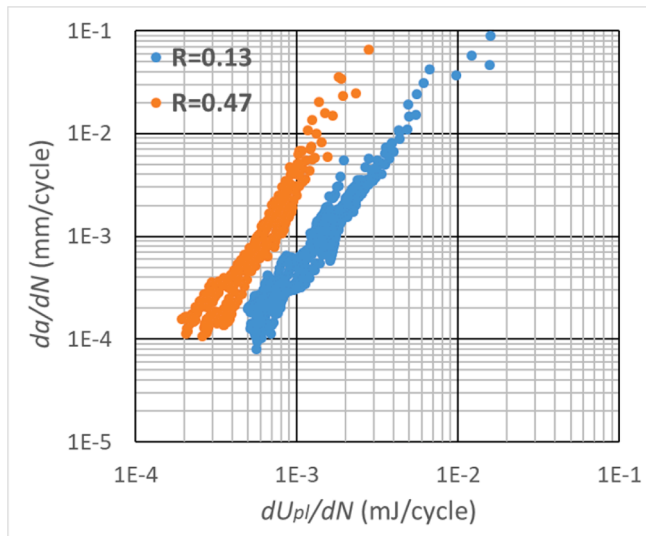**Fig. 14.** The dU_{pl}/dN-$\Delta\sqrt{G}$ relationship.

Fig. 15. The dU_{pl}/dN - da/dN relationship.

of the change in elastic strain energy throughout one full cycle dU_e/dN, the plastic dissipation per cycle dU_{pl}/dN and the surface energy dissipated dU_a/dN. Fatigue tests of DCB Mode I tests of adhesive joints with adhesive FM94 and 7075-T6 adherend were carried out to unravel the relationship between da/dN and energy variables. It is concluded that only the surface forming energy dU_a/dN, which is independent of stress ratio and specimen type, is straightforwardly linked to fatigue crack growth, while dU_e/dN and dU_{pl}/dN are only consequences accompanying fatigue crack growth.

Undoubtedly, this paper has limitations. Firstly, dU_{pl}/dN and dU_a/dN were obtained numerically, without directly measured from experiments. Secondly, the real fracture surface area A considering the surface roughness should be correlated with energy variables instead of the flat planar surface, which was considered in this paper to be proportional to the crack length. Finally, the values of dU_a/dN shown here are a first approximation to reveal the trend, with the assumptions of crack growth in certain patterns and flat fracture surface. Therefore, future work is needed for obtaining more accurate results for the energy variables. Despite the limitations, it is clear that scientifically the dU_e/dN- da/dN relationship and the dU_{pl}/dN- da/dN relationship are both indirectly related to crack growth. Hence, when using the parameters derived from strain energy release and plastic dissipation to predict fatigue crack growth in adhesive joints, one should keep in mind that the relation
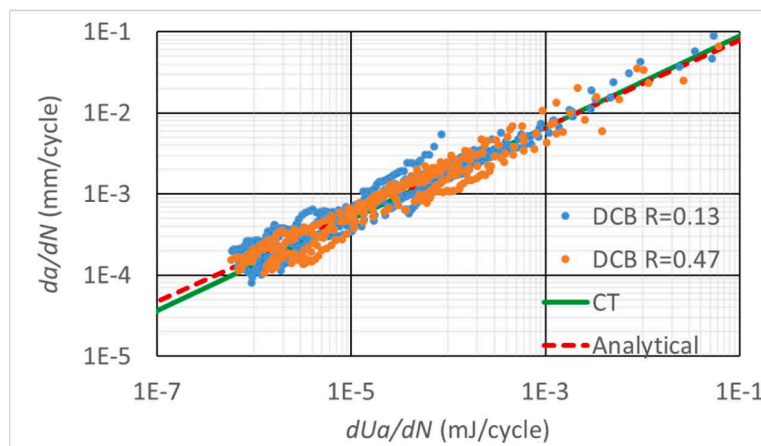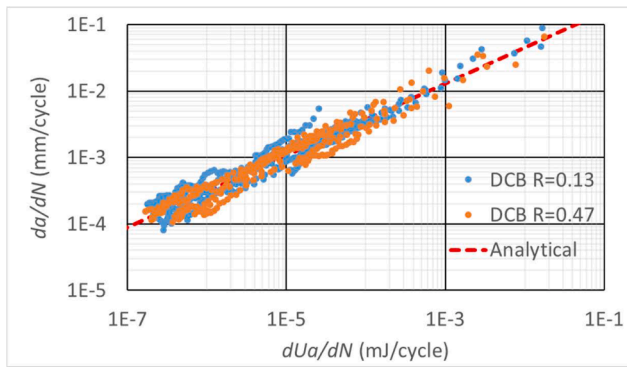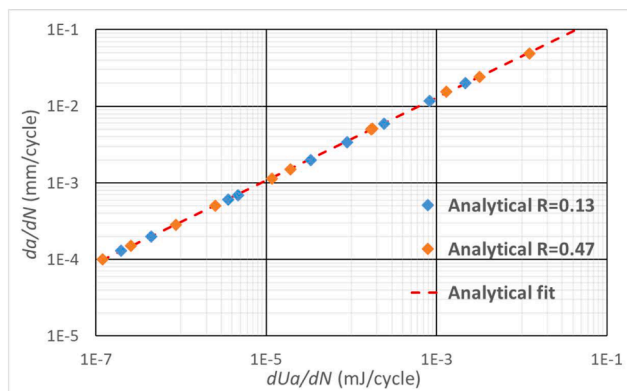

(a) dU_a/dN-*da/dN* relationship for DCB specimen
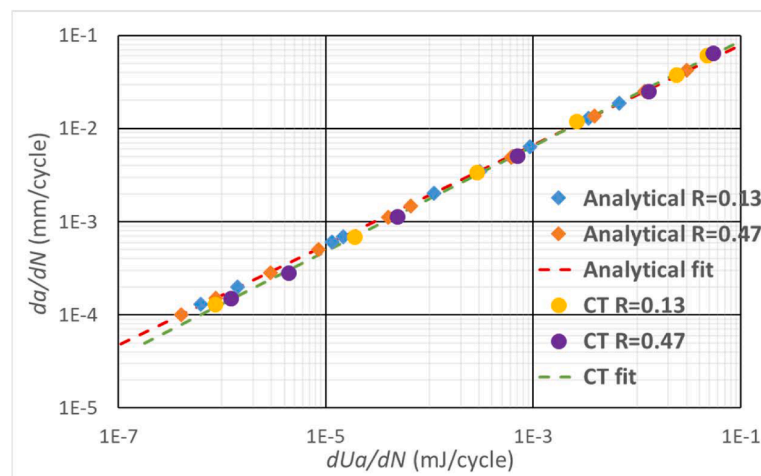
(b) dU_a/dN-*da/dN* relationship from FEA CT specimen and from analytical approach

Fig. 16. The relation between dU_a/dN and da/dN for Pattern A.

(a) dU_a/dN-da/dN relationship for DCB specimen

(b) dU_a/dN-da/dN relationship from analytical approach

Fig. 17. The relation between dU_a/dN and da/dN for Pattern B.

between these parameters and da/dN can be different among different load and specimen geometry conditions.

Declaration of Competing Interest

The authors declare that they have no known competing financial interests or personal relationships that could have appeared to influence the work reported in this paper.

References

[1] M. Shahverdi, A.P. Vassilopoulos, T. Keller, A total fatigue life model for the prediction of the R-ratio effects on fatigue crack growth of adhesively-bonded pultruded GFRP DCB joints, Compos. A Appl. Sci. Manuf. 43 (10) (2012) 1783–1790.

[2] M. Shahverdi, A.P. Vassilopoulos, T. Keller, Experimental investigation of R-ratio effects on fatigue crack growth of adhesively-bonded pultruded GFRP DCB joints under CA loading, Compos. A Appl. Sci. Manuf. 43 (10) (2012) 1689–1697.

[3] A. Pirondi, G. Nicoletto, Mixed mode I/II fatigue crack growth in adhesive joints, Eng. Fract. Mech. 73 (16) (2006) 2557–2568.

[4] S. Erpolat, I.A. Ashcroft, A.D. Crocombe, M.M. Abdel-Wahab, Fatigue crack growth acceleration due to intermittent overstressing in adhesively bonded CFRP joints, Compos. A Appl. Sci. Manuf. 35 (10) (2004) 1175–1183.

[5] M. Imanaka, K. Ishii, K. Hara, T. Ikeda, Y. Kouno, Fatigue crack propagation rate of CFRP/aluminum adhesively bonded DCB joints with acrylic and epoxy adhesives, Int. J. Adhes. Adhes. 85 (2018) 149–156.

[6] L. Adamos, T. Loutas, Challenges in the fatigue crack growth characterization of metal/composite joints: A compliance-based investigation of a Ti/CFRP joint, Int. J. Fatigue 148 (2021) 106233, https://doi.org/10.1016/j.ijfatigue.2021.106233.

[7] Q. Chen, H. Guo, K. Avery, H. Kang, X. Su, Mixed-mode fatigue crack growth and life prediction of an automotive adhesive bonding system, Eng. Fract. Mech. 189 (2018) 439–450.

[8] Y. Liu, S. Lemanski, X. Zhang, D. Ayre, H.Y. Nezhad, A finite element study of fatigue crack propagation in single lap bonded joint with process-induced disbond, Int. J. Adhes. Adhes. 87 (2018) 164–172.

[9] G. Clerc, A.J. Brunner, S. Josset, P. Niemz, F. Pichelin, J.W.G. Van de Kuilen, Adhesive wood joints under quasi-static and cyclic fatigue fracture Mode II loads, Int. J. Fatigue 123 (2019) 40–52.

[10] I. Floros, K. Tserpes, Fatigue crack growth characterization in adhesive CFRP joints, Compos. Struct. 207 (2019) 531–536.

[11] Griffith, Alan Arnold. "VI. The phenomena of rupture and flow in solids." Philosophical transactions of the royal society of London. Series A, containing papers of a mathematical or physical character 221.582–593 (1921), 163–198.

[12] Irwin, G. R. "Relation of stresses near a crack to the crack extension force." 9th Cong. App. Mech., Brussels (1957).

[13] J.A. Pascoe, R.C. Alderliesten, R. Benedictus, On the relationship between disbond growth and the release of strain energy, Eng. Fract. Mech. 133 (2015) 1–13.

[14] M. Mazari, B. Bouchouicha, M. Zemri, M. Benguediab, N. Ranganathan, Fatigue crack propagation analyses based on plastic energy approach, Comput. Mater. Sci. 41 (3) (2008) 344–349.

[15] K.V. Smith, Application of the dissipated energy criterion to predict fatigue crack growth of Type 304 stainless steel following a tensile overload, Eng. Fract. Mech. 78 (18) (2011) 3183–3195.

[16] N. Klingbeil, A total dissipated energy theory of fatigue crack growth in ductile solids, Int. J. Fatigue 25 (2) (2003) 117–128.

[17] C.M. Baudendistel, N.W. Klingbeil, Effect of a graded layer on the plastic dissipation in mixed-mode fatigue crack growth along plastically mismatched interfaces, Int. J. Fatigue 51 (2013) 96–104.

[18] P.G. Nittur, A.M. Karlsson, L.A. Carlsson, Numerical evaluation of Paris-regime crack growth rate based on plastically dissipated energy, Eng. Fract. Mech. 124-125 (2014) 155–166.

[19] A.N. Vshivkov, A.Y. Iziumova, I.A. Panteleev, A.V. Ilinykh, V.E. Wildemann, O. A. Plekhov, The study of a fatigue crack propagation in titanium Grade 2 using analysis of energy dissipation and acoustic emission data, Eng. Fract. Mech. 210 (2019) 312–319.

[20] G. Meneghetti, M. Ricotta, A heat energy dissipation approach to elastic-plastic fatigue crack propagation, Theor. Appl. Fract. Mech. 105 (2020) 102405, https://doi.org/10.1016/j.tafmec.2019.102405.

[21] D. Palumbo, R. De Finis, F. Ancona, U. Galietti, Damage monitoring in fracture mechanics by evaluation of the heat dissipated in the cyclic plastic zone ahead of the crack tip with thermal measurements, Eng. Fract. Mech. 181 (2017) 65–76.

[22] L. Yao, R.C. Alderliesten, M. Zhao, R. Benedictus, Discussion on the use of the strain energy release rate for fatigue delamination characterization, Compos. A Appl. Sci. Manuf. 66 (2014) 65–72.

[23] L. Yao, Y.i. Sun, L. Guo, X. Lyu, M. Zhao, L. Jia, R.C. Alderliesten, R. Benedictus, Mode I fatigue delamination growth with fibre bridging in multidirectional composite laminates, Eng. Fract. Mech. 189 (2018) 221–231.

[24] L. Amaral, D. Zarouchas, R. Alderliesten, R. Benedictus, Energy dissipation in mode II fatigue crack growth, Eng. Fract. Mech. 173 (2017) 41–54.

[25] L. Amaral, R. Alderliesten, R. Benedictus, Understanding mixed-mode cyclic fatigue delamination growth in unidirectional composites: An experimental approach, Eng. Fract. Mech. 180 (2017) 161–178.

[26] S.i. Xiao, H.-L. Wang, B. Liu, K.-C. Hwang, The surface-forming energy release rate based fracture criterion for elastic–plastic crack propagation, J. Mech. Phys. Solids 84 (2015) 336–357.

[27] Y. Bai, T. Guo, J. Wang, J. Gao, K. Gao, X. Pang, Stress-sensitive fatigue crack initiation mechanisms of coated titanium alloy, Acta Mater. 217 (2021) 117179, https://doi.org/10.1016/j.actamat.2021.117179.

[28] ASTM. E647 Standard Test Method for Measurement of Fatigue Crack Growth Rates. West Conshohocken, PA: ASTM International; 2015.

[29] H. Quan, R. Alderliesten, On the effect of plastic model on simulation of adhesive bonded joints with FM94, Int. J. Adhes. Adhes. 110 (2021) 102916, https://doi.org/10.1016/j.ijadhadh.2021.102916.

[30] J.C. Newman, A crack-closure model for predicting fatigue crack growth under aircraft spectrum loading, Methods and models for predicting fatigue crack growth under random loading, ASTM International, 1981.

[31] Pascoe, John-Alan. "Characterisation of fatigue crack growth in adhesive bonds." Delft University of Technology. (2016).

[32] J.A. Pascoe, R.C. Alderliesten, R. Benedictus, On the physical interpretation of the R-ratio effect and the LEFM parameters used for fatigue crack growth in adhesive bonds, Int. J. Fatigue 97 (2017) 162–176.

[33] Bürger, D. B. "Mixed-mode fatigue disbond on metallic bonded joints." (2015)." Delft University of Technology. (2015).

[34] D. Bürger, C.D. Rans, R. Benedictus, Influence of fabric carrier on the fatigue disbond behavior of metal-to-metal bonded interfaces, J. Adhesion 90 (5-6) (2014) 482–495.

[35] N. Ranganathan, F. Chalon, S. Meo, Some aspects of the energy based approach to fatigue crack propagation, Int. J. Fatigue 30 (10-11) (2008) 1921–1929.

[36] Gwider, A. "Contribution to the Applicability of Energy Based concepts for Fatigue Crack Propagation." University of Tours (2019).

[37] X.G. Wang, H.R. Ran, C. Jiang, Q.H. Fang, An energy dissipation-based fatigue crack growth model, Int. J. Fatigue 114 (2018) 167–176.